PHYSICAL REVIEW D **76,** 011104(R) (2007)

Improved measurement of CP-violating parameters in $B \to \rho^+\rho^-$ decays

A. Somov,[2] A. J. Schwartz,[2] I. Adachi,[7] H. Aihara,[42] D. Anipko,[1] V. Aulchenko,[1] T. Aushev,[11,16] A. M. Bakich,[37] I. Bedny,[1] U. Bitenc,[12] I. Bizjak,[12] A. Bondar,[1] M. Bračko,[7,12,18] T. E. Browder,[6] M.-C. Chang,[3] Y. Chao,[24] A. Chen,[22] K.-F. Chen,[24] W. T. Chen,[22] B. G. Cheon,[5] R. Chistov,[11] I.-S. Cho,[47] Y. Choi,[36] Y. K. Choi,[36] S. Cole,[37] J. Dalseno,[19] M. Dash,[46] J. Dragic,[7] A. Drutskoy,[2] S. Eidelman,[1] S. Fratina,[12] G. Gokhroo,[38] B. Golob,[12,17] H. Ha,[14] J. Haba,[7] T. Hara,[29] K. Hayasaka,[20] H. Hayashii,[21] M. Hazumi,[7] D. Heffernan,[29] T. Hokuue,[20] Y. Hoshi,[40] W.-S. Hou,[24] H. J. Hyun,[15] T. Iijima,[20] K. Inami,[20] A. Ishikawa,[42] H. Ishino,[43] R. Itoh,[7] M. Iwasaki,[42] Y. Iwasaki,[7] N. Joshi,[38] D. H. Kah,[15] J. H. Kang,[47] N. Katayama,[7] H. Kichimi,[7] H. O. Kim,[36] Y. J. Kim,[4] K. Kinoshita,[2] S. Korpar,[12,18] P. Križan,[12,17] P. Krokovny,[7] R. Kulasiri,[2] R. Kumar,[30] C. C. Kuo,[22] A. Kuzmin,[1] Y.-J. Kwon,[47] J. S. Lee,[36] M. J. Lee,[35] S. E. Lee,[35] T. Lesiak,[25] A. Limosani,[7] S.-W. Lin,[24] D. Marlow,[32] T. Matsumoto,[44] S. McOnie,[37] T. Medvedeva,[11] W. Mitaroff,[9] H. Miyake,[29] H. Miyata,[27] Y. Miyazaki,[20] R. Mizuk,[11] D. Mohapatra,[46] G. R. Moloney,[19] M. Nakao,[7] O. Nitoh,[45] T. Nozaki,[7] S. Ogawa,[39] T. Ohshima,[20] S. Okuno,[13] S. L. Olsen,[6] Y. Onuki,[33] H. Ozaki,[7] P. Pakhlov,[11] G. Pakhlova,[11] C. W. Park,[36] R. Pestotnik,[12] L. E. Piilonen,[46] H. Sahoo,[6] Y. Sakai,[7] O. Schneider,[16] J. Schümann,[7] K. Senyo,[20] M. Shapkin,[10] C. P. Shen,[8] H. Shibuya,[39] B. Shwartz,[1] M. Starič,[12] H. Stoeck,[37] K. Sumisawa,[7] T. Sumiyoshi,[44] F. Takasaki,[7] N. Tamura,[27] M. Tanaka,[7] Y. Teramoto,[28] X. C. Tian,[31] K. Trabelsi,[7] T. Tsukamoto,[7] S. Uehara,[7] K. Ueno,[24] T. Uglov,[11] Y. Unno,[5] S. Uno,[7] P. Urquijo,[19] Y. Usov,[1] G. Varner,[6] K. E. Varvell,[37] S. Villa,[16] A. Vinokurova,[1] C. C. Wang,[24] C. H. Wang,[23] M.-Z. Wang,[24] P. Wang,[8] Y. Watanabe,[43] E. Won,[14] B. D. Yabsley,[37] A. Yamaguchi,[41] Y. Yamashita,[26] Z. P. Zhang,[34] and A. Zupanc[12]

(Belle Collaboration)

[1]*Budker Institute of Nuclear Physics, Novosibirsk*
[2]*University of Cincinnati, Cincinnati, Ohio 45221, USA*
[3]*Department of Physics, Fu Jen Catholic University, Taipei*
[4]*The Graduate University for Advanced Studies, Hayama*
[5]*Hanyang University, Seoul*
[6]*University of Hawaii, Honolulu, Hawaii 96822, USA*
[7]*High Energy Accelerator Research Organization (KEK), Tsukuba*
[8]*Institute of High Energy Physics, Chinese Academy of Sciences, Beijing*
[9]*Institute of High Energy Physics, Vienna*
[10]*Institute of High Energy Physics, Protvino*
[11]*Institute for Theoretical and Experimental Physics, Moscow*
[12]*J. Stefan Institute, Ljubljana*
[13]*Kanagawa University, Yokohama*
[14]*Korea University, Seoul*
[15]*Kyungpook National University, Taegu*
[16]*Swiss Federal Institute of Technology of Lausanne, EPFL, Lausanne*
[17]*University of Ljubljana, Ljubljana*
[18]*University of Maribor, Maribor*
[19]*University of Melbourne, School of Physics, Victoria 3010*
[20]*Nagoya University, Nagoya*
[21]*Nara Women's University, Nara*
[22]*National Central University, Chung-li*
[23]*National United University, Miao Li*
[24]*Department of Physics, National Taiwan University, Taipei*
[25]*H. Niewodniczanski Institute of Nuclear Physics, Krakow*
[26]*Nippon Dental University, Niigata*
[27]*Niigata University, Niigata*
[28]*Osaka City University, Osaka*
[29]*Osaka University, Osaka*
[30]*Panjab University, Chandigarh*
[31]*Peking University, Beijing*
[32]*Princeton University, Princeton, New Jersey 08544, USA*
[33]*RIKEN BNL Research Center, Upton, New York 11973, USA*
[34]*University of Science and Technology of China, Hefei*
[35]*Seoul National University, Seoul*

[36]*Sungkyunkwan University, Suwon*
[37]*University of Sydney, Sydney, New South Wales*
[38]*Tata Institute of Fundamental Research, Mumbai*
[39]*Toho University, Funabashi*
[40]*Tohoku Gakuin University, Tagajo*
[41]*Tohoku University, Sendai*
[42]*Department of Physics, University of Tokyo, Tokyo*
[43]*Tokyo Institute of Technology, Tokyo*
[44]*Tokyo Metropolitan University, Tokyo*
[45]*Tokyo University of Agriculture and Technology, Tokyo*
[46]*Virginia Polytechnic Institute and State University, Blacksburg, Virginia 24061, USA*
[47]*Yonsei University, Seoul*

(Received 1 May 2007; published 10 July 2007)

We present a measurement of the *CP*-violating asymmetry in $B^0 \to \rho^+\rho^-$ decays using 535×10^6 $B\bar{B}$ pairs collected with the Belle detector at the KEKB e^+e^- collider. We measure *CP*-violating coefficients $\mathcal{A} = 0.16 \pm 0.21(\text{stat}) \pm 0.08(\text{syst})$ and $\mathcal{S} = 0.19 \pm 0.30(\text{stat}) \pm 0.08(\text{syst})$. These values are used to determine the unitarity triangle angle ϕ_2 using an isospin analysis; the solution consistent with the standard model lies in the range $54° < \phi_2 < 113°$ at the 90% confidence level.

DOI: 10.1103/PhysRevD.76.011104 PACS numbers: 13.25.Hw, 11.30.Er, 12.15.Hh

CP violation in the standard model is attributed to the presence of an irreducible complex phase in the Cabibbo-Kobayashi-Maskawa [1] (CKM) quark-mixing matrix. The unitarity of the CKM matrix leads to six triangles in the complex plane. One such triangle is given by the following relation among the matrix elements: $V_{ud}V_{ub}^* + V_{cd}V_{cb}^* + V_{td}V_{tb}^* = 0$. The phase angle ϕ_2, defined as $\arg[-(V_{td}V_{tb}^*)/(V_{ud}V_{ub}^*)]$, can be determined by measuring a time-dependent *CP* asymmetry in $b \to u\bar{u}d$ decays such as $B^0 \to \pi^+\pi^-$, $(\rho\pi)^0$, and $\rho^+\rho^-$ [2]. The time-dependent rate for $B \to \rho^+\rho^-$ decays tagged with B^0 ($Q = +1$) and $\bar{B}^0$ ($Q = -1$) mesons is given by

$$\mathcal{P}_{\rho\rho}(\Delta t) = \frac{e^{-|\Delta t|/\tau_{B^0}}}{4\tau_{B^0}}\{1 + Q[\mathcal{A}\cos(\Delta m \Delta t) + \mathcal{S}\sin(\Delta m \Delta t)]\}, \quad (1)$$

where τ_{B^0} is the B^0 lifetime, Δm is the mass difference between the two B^0 mass eigenstates, Δt is the proper-time difference between the two B decays in the event, and $\mathcal{A}$ and $\mathcal{S}$ are *CP* asymmetry coefficients. If the decay amplitude is a pure *CP*-even state and is dominated by a tree diagram, $\mathcal{S} = \sin(2\phi_2)$ and $\mathcal{A} = 0$. The presence of an amplitude with a different weak phase (such as from a gluonic penguin diagram) gives rise to direct *CP* violation and shifts $\mathcal{S}$ from $\sin(2\phi_2)$. However, the size of a penguin amplitude is constrained to be small with respect to the leading tree diagram by the small branching fraction of $B^0 \to \rho^0\rho^0$ [3].

The *CP*-violating parameters receive contributions from a longitudinally polarized state (*CP*-even) and two transversely polarized states (an admixture of *CP*-even and *CP*-odd states). Recent measurements of the polarization fraction by Belle [4] and *BABAR* [5] show that the longitudinal polarization fraction is near unity ($f_L = 0.968 \pm 0.023$ [6]).

Here we present an improved measurement of the *CP*-violating coefficients $\mathcal{A}$ and $\mathcal{S}$ using 492 fb^{-1} of data containing 535×10^6 $B\bar{B}$ pairs. This data sample is about a factor of 2 larger than that used in our earlier publication [4]. In addition, we have modified the event selection by reducing the threshold on a continuum suppression variable; this increases our reconstruction efficiency by about 70%. We subsequently introduce a probability density function (PDF) for the continuum suppression variable into the likelihood function; this provides additional discrimination between signal and backgrounds. The improvement in the statistical error of $\mathcal{A}$ and $\mathcal{S}$ predicted by Monte Carlo (MC) simulation due to the new event selection is about 12%.

The $B\bar{B}$ pairs were collected with the Belle detector [7] at the KEKB [8] e^+e^- asymmetric-energy (3.5 GeV on 8.0 GeV) collider with a center-of-mass (CM) energy at the $\Upsilon(4S)$ resonance. The $\Upsilon(4S)$ is produced with a Lorentz boost of $\beta\gamma = 0.425$ nearly along the z axis, which is oriented antiparallel to the positron beam. Since the B^0 and $\bar{B}^0$ mesons are produced approximately at rest in the $\Upsilon(4S)$ CM system, the decay time difference Δt is related to the distance between the decay vertices of the two B mesons as $\Delta t \simeq \Delta z/\beta\gamma c$, where c is the speed of light.

The Belle detector [7] is a large-solid-angle spectrometer. It includes a silicon vertex detector (SVD), a 50-layer central drift chamber (CDC), an array of aerogel threshold Cherenkov counters (ACC), time-of-flight scintillation counters (TOF), and an electromagnetic calorimeter (ECL) comprised of CsI(Tl) crystals located inside a superconducting solenoid coil that provides a 1.5 T magnetic field.

We reconstruct $B^0 \to \rho^+\rho^-$ decays by combining two oppositely charged pion tracks with two neutral pions. Each charged track is required to have a transverse momentum $p_T > 0.10$ GeV/c in the laboratory frame and

originate within $dr < 0.2$ cm in the radial direction and within $|dz| < 4.0$ cm along the z-axis from the interaction point, which is determined run by run. A track is identified as a pion using information from the CDC, ACC, and TOF systems. Tracks matched with clusters in the ECL that are consistent with an electron hypothesis are rejected.

The π^0 candidates are reconstructed from $\gamma\gamma$ pairs with an invariant mass in the range $117.8\ \mathrm{MeV}/c^2 < M_{\gamma\gamma} < 150.2\ \mathrm{MeV}/c^2$ (about $\pm 3\sigma$ in m_{π^0} resolution). Photons are required to have energy $E_\gamma > 50$ MeV in the ECL barrel region ($32° < \theta < 129°$) and $E_\gamma > 90$ MeV in the end cap regions ($17° < \theta < 32°$ and $129° < \theta < 150°$), where θ denotes the polar angle with respect to the z axis.

To reconstruct $\rho^\pm$ mesons, we combine $\pi^\pm$ candidates with π^0 candidates. The $\pi^\pm\pi^0$ combination must have an invariant mass in the range $0.62\ \mathrm{GeV}/c^2 < M_{\pi^\pm\pi^0} < 0.92\ \mathrm{GeV}/c^2$. To reduce combinatorial background with low momentum π^0's, we reject π^0's with $p < 0.35\ \mathrm{GeV}/c$ in the CM frame. We also require $-0.80 < \cos\theta_\pm < 0.98$, where $\theta_\pm$ is the angle between the direction of the π^0 from the $\rho^\pm$ and the direction opposite the B^0 momentum in the $\rho^\pm$ rest frame. This requirement decreases backgrounds arising from spurious combinations of low momentum π^0's which lead to $\cos\theta_\pm$ values near -1.

$B^0 \to \rho^+\rho^-$ decays are identified using the beam-energy-constrained mass $M_{\mathrm{bc}} \equiv \sqrt{E^2_{\mathrm{beam}} - p^2_B}$ and energy difference $\Delta E \equiv E_B - E_{\mathrm{beam}}$, where E_{beam} is the beam energy, and E_B and p_B are the energy and momentum of the reconstructed B candidate, all evaluated in the CM frame.

The flavor of the B meson accompanying the $B^0 \to \rho^+\rho^-$ candidate is identified via its decay products: charged leptons, kaons, and Λ's. A tagging algorithm [9] yields the flavor of the tagged meson, Q, and a quality factor, r. The parameter r ranges from 0 for no flavor discrimination to 1 for unambiguous flavor assignment. We divide the data sample into six r intervals (denoted $\ell = 1, 2, \ldots, 6$). The wrong tag fractions ω_ℓ for these intervals and the differences $\Delta\omega_\ell$ in these fractions between B^0 and $\bar{B}^0$ decays are determined from data [9].

The dominant background originates from $e^+e^- \to q\bar{q}$ ($q = u, d, s, c$) continuum events. To separate $q\bar{q}$ jetlike events from more spherical $B\bar{B}$ events, we use event-shape variables, specifically, 16 modified Fox-Wolfram moments [10] combined into a Fisher discriminant [11]. We form signal and background likelihood functions $\mathcal{L}_s$ and $\mathcal{L}_{\mathrm{BG}}$ by multiplying the PDF for the Fisher discriminant by a PDF for $\cos\theta_B$, where θ_B is the polar angle in the CM frame between the B direction and the beam axis. The PDFs for signal and $q\bar{q}$ are obtained from MC simulations and the data sideband $5.23\ \mathrm{GeV}/c^2 < M_{\mathrm{bc}} < 5.26\ \mathrm{GeV}/c^2$, respectively. We calculate the ratio $\mathcal{R} = \mathcal{L}_s/(\mathcal{L}_s + \mathcal{L}_{\mathrm{BG}})$ and make a loose requirement $\mathcal{R} > 0.15$.

The decay vertices of a $\rho^+\rho^-$ candidate and the tag-side B meson are reconstructed using charged tracks that have a sufficient number of SVD hits and an interaction point constraint. The vertex reconstruction algorithm is described in Ref. [12].

The analysis is organized in two main steps. We first determine the yields of signal and background components from a fit to the three-dimensional (M_{bc}, ΔE, $\mathcal{R}$) distribution. Here, B^0 candidates are required to satisfy $5.23\ \mathrm{GeV}/c^2 < M_{\mathrm{bc}} < 5.29\ \mathrm{GeV}/c^2$, $-0.2\ \mathrm{GeV} < \Delta E < 0.26\ \mathrm{GeV}$, and $\mathcal{R} > 0.15$. We subsequently perform a fit to the Δt distribution to determine the CP parameters $\mathcal{A}$ and $\mathcal{S}$. The signal region used for the Δt fit is $5.27\ \mathrm{GeV}/c^2 < M_{\mathrm{bc}} < 5.29\ \mathrm{GeV}/c^2$, $-0.12\ \mathrm{GeV} < \Delta E < 0.08\ \mathrm{GeV}$, and $\mathcal{R} > 0.15$.

About 12.6% of events contain multiple $B^0 \to \rho^+\rho^-$ candidates, most of which arise from fake π^0's combining with good tracks. We select the best candidate based on the π^0 masses, i.e., minimizing $\sum_{\pi^0_{1,2}}(m_{\gamma\gamma} - m_{\pi^0})^2$. After this selection, some multiple candidates remain due to combinations of extraneous $\pi^\pm$ tracks with a single π^0. Such events constitute about 3% of the total number of events, and for these events we select one candidate randomly. Signal decays that have at least one π meson incorrectly identified are referred to as "self-cross-feed" (SCF) events.

The likelihood function used to determine the event yields is given by

$$\mathcal{L} = \exp\left(-\sum_j N_j\right)\prod_{i=1}^{N_{\mathrm{evt}}}\left[\sum_j N_j \mathcal{P}_j(M^i_{\mathrm{bc}}, \Delta E^i, \mathcal{R}^i)\right], \quad (2)$$

where j indicates one of the following event categories: signal and $\rho\pi\pi$ nonresonant decays, SCF events, continuum background ($q\bar{q}$), $b \to c$ background, and charmless ($b \to u$) background. N_j is the yield of each category, $\mathcal{P}_j(M^i_{\mathrm{bc}}, \Delta E^i, \mathcal{R}^i)$ is the PDF for the ith event for category j, and N_{evt} is the total number of events in the fit. Except for the contributions of $b \to u$ background and SCF events, the yields N_j are determined from the fit. Because of the similar shapes of the M_{bc}, ΔE, and $\mathcal{R}$ distributions for signal and $\rho\pi\pi$ events, we cannot distinguish these two components; the fraction of $\rho\pi\pi$ events is measured in Ref. [4] and constitutes $(6.3 \pm 6.7)\%$ of the total $N_{\rho^+\rho^- + \rho\pi\pi}$ signal. The fraction of SCF events is determined from MC simulation to be 32.1% of all signal events and is fixed in the fit. The M_{bc} and ΔE shapes for the signal and SCF components are modeled by a two-dimensional smoothed histogram obtained from a large MC sample. To take into account a small difference between the MC and data, the M_{bc}-ΔE shapes are corrected according to calibration factors determined from a $B^+ \to \bar{D}^0\rho^+$, $\bar{D}^0 \to K^+\pi^-\pi^0$ control sample. The $\mathcal{R}$ shapes are modeled by one-dimensional histograms, also obtained from MC simulation.

The PDF for $b \to c$ background is the product of a threshold ARGUS function [13] for M_{bc}, a quadratic poly-

nomial for ΔE, and the sum of a Gaussian and a third-order polynomial for $\mathcal{R}$. The shapes of the ΔE and $\mathcal{R}$ distributions depend on the tag quality bin ℓ. Parameters for all distributions are obtained from the MC.

The $M_{\rm bc}$ and ΔE PDFs for $q\bar{q}$ are modeled by an ARGUS function and a linear function, respectively. The ΔE slope depends on $\mathcal{R}$ and the tag quality bin ℓ. The shape parameters for $M_{\rm bc}$ and ΔE are floated in the fit. The $\mathcal{R}$ PDF for $q\bar{q}$ background is taken to be an eighth-order polynomial function; the coefficients depend on the bin ℓ and are determined from a data sample collected at a CM energy $\sim$60 MeV below the $\Upsilon(4S)$.

The $b \to u$ background is dominated by $B \to (\rho\pi, a_1\pi, a_1\rho)$ decays. We estimate the $B^{\pm} \to (a_1\pi)^{\pm}$ branching fractions (which are unmeasured) to be $(20 \pm 10) \times 10^{-6}$ using the measured value for $B^0 \to a_1^{\pm}\pi^{\mp}$ [14]. For $B^{\pm} \to (a_1\rho)^{\pm}$ we assume branching fractions of $(30 \pm 15) \times 10^{-6}$, consistent with the present upper limit for $B^0 \to a_1^{\pm}\rho^{\mp}$ ($< 6 \times 10^{-5}$ [15]). The fraction of $b \to u$ events is very small (0.37%) and thus is fixed in the fit according to the prediction of MC simulation. A fit to 176 843 events maximizing $\mathcal{L}$ yields $N_{\rho\rho+\rho\pi\pi} = 576 \pm 53$. Figures 1 and 2 show the $M_{\rm bc}$, ΔE, and $\mathcal{R}$ distributions along with projections of the fit result.

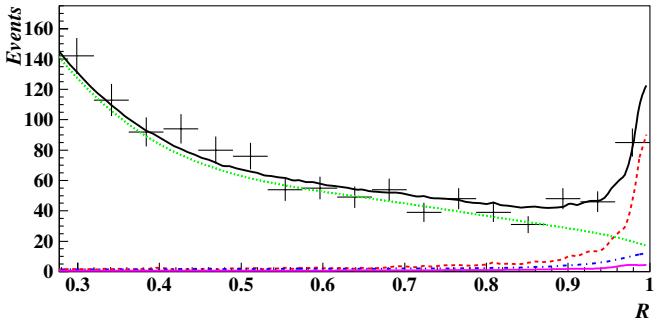

FIG. 2 (color online). $\mathcal{R}$ distribution for high-purity tagged events satisfying $5.27\ \text{GeV}/c^2 < M_{\rm bc} < 5.29\ \text{GeV}/c^2$ and $-0.10\ \text{GeV} < \Delta E < 0.06\ \text{GeV}$. The curves show fit projections: dashed is $\rho^+\rho^- + \rho\pi\pi$, dotted is $q\bar{q}$, dot-dashed is $b \to c$, small solid is $b \to u$, and large solid is the total.

The CP-violating parameters $\mathcal{A}$ and $\mathcal{S}$ are obtained using an unbinned ML fit to the Δt distribution. The likelihood function for event i is given by

$$\mathcal{L}_i = \sum_n \int f_n(\vec{x}_i)\mathcal{P}_n(\Delta t')R_n(\Delta t^i, \Delta t')d\Delta t', \qquad (3)$$

where n is one of the six event categories: correctly re-

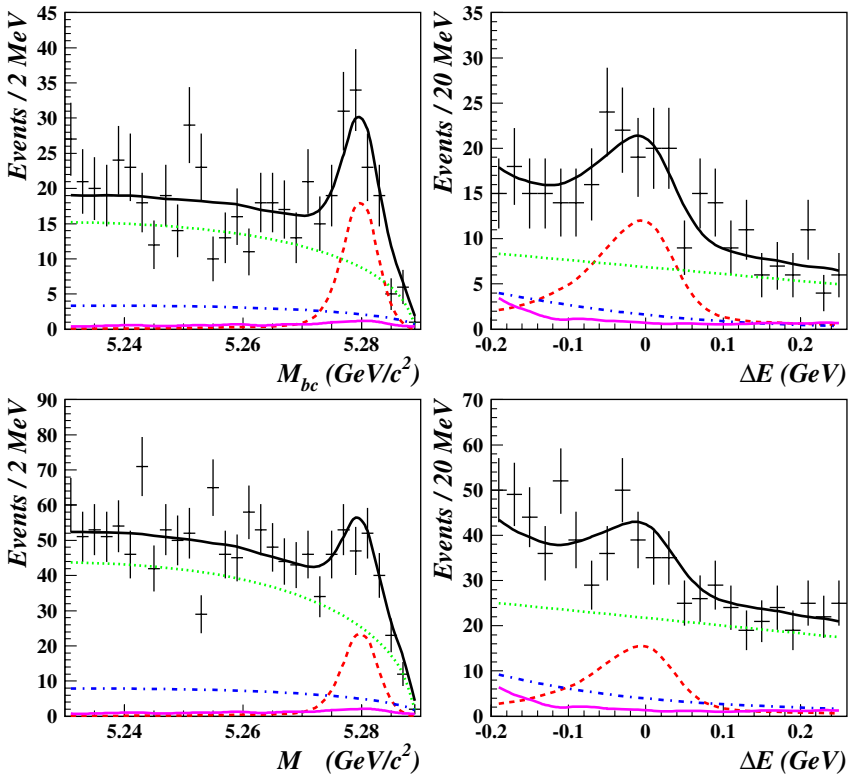

FIG. 1 (color online). Left: projections in $M_{\rm bc}$ for events satisfying $-0.10\ \text{GeV} < \Delta E < 0.06\ \text{GeV}$. Right: projections in ΔE for events with $5.27\ \text{GeV}/c^2 < M_{\rm bc} < 5.29\ \text{GeV}/c^2$. The top plots correspond to good quality tags ($0.75 < r < 1.0$), and the bottom plots correspond to lower quality tags ($r < 0.75$). The curves show fit projections: dashed is $\rho^+\rho^- + \rho\pi\pi$, dotted is $q\bar{q}$, dot-dashed is $b \to c$, small solid is $b \to u$, and large solid is the total. For these plots the $\mathcal{R}$ requirement has been tightened to increase the ratio of signal to background.

constructed signal, SCF events, $\rho\pi\pi$ nonresonant events, $b \to c$ background, $q\bar{q}$ background, and $b \to u$ background. The weights f_n are functions of $\vec{x} \in (M_{\rm bc}, \Delta E, \mathcal{R})$ and are normalized to the event fractions obtained from the $(M_{\rm bc}, \Delta E, \mathcal{R})$ fit. The PDFs $\mathcal{P}_n(\Delta t)$ are convolved with the corresponding Δt resolution functions R_n. Both f_n and $\mathcal{P}_n(\Delta t)$ depend on the tag quality bin ℓ.

The signal PDF is given by Eq. (1) modified to take into account the effect of incorrect flavor assignment: $e^{-|\Delta t|/\tau_{B^0}}/(4\tau_{B^0}) \times \{1 - Q\Delta\omega_\ell + Q(1-2\omega_\ell)[\mathcal{A}\cos(\Delta m\Delta t) + \mathcal{S}\sin(\Delta m\Delta t)]\}$. As the fraction of longitudinal polarization f_L is close to 100%, we assume that $\mathcal{A} = \mathcal{A}_L, \mathcal{S} = \mathcal{S}_L$, and consider the potential contribution from a transversely polarized amplitude as a systematic uncertainty. The signal PDF is convolved with the same Δt resolution function as that used for Belle's $\sin 2\phi_1$ measurement [12].

The fraction of SCF events with incorrectly reconstructed vertices is estimated from MC simulation to be $(6.5 \pm 0.1)\%$ of all signal events. The PDFs $\mathcal{P}_{\rho\pi\pi}$ and $\mathcal{P}_{\rm SCF}$ are exponential with $\tau = \tau_B$ and $\tau \approx 0.96$ ps (from MC), respectively; these are smeared by a common resolution function.

The Δt PDFs for the backgrounds are modeled as a sum of prompt and exponential components: $\mathcal{P}_k = f_\delta^k \delta(\Delta t) + (1 - f_\delta^k) e^{-|\Delta t|/\tau_k}/2\tau_k$, where k represents continuum, $b \to c$, and $b \to u$ backgrounds, f_δ^k is the fraction of the prompt component, $\delta(\Delta t)$ is the Dirac delta function, and τ_k is an effective lifetime. These PDFs are convolved with a resolutionlike function R_k parametrized as a sum of two Gaussian functions. Parameters for $\mathcal{P}_k$ and R_k are determined from a data sideband for continuum background and from large MC samples for $b \to c$ and $b \to u$ backgrounds. To account for small correlations between the shape of the Δt distribution and $\mathcal{R}$ for $q\bar{q}$ background, the parameters are obtained separately for low $(0.15 < \mathcal{R} < 0.75)$ and high $(0.75 < \mathcal{R} < 1.0)$ $\mathcal{R}$ regions.

We determine $\mathcal{A}$ and $\mathcal{S}$ by maximizing $\sum_i \log \mathcal{L}_i$, where i runs over the 18 016 events in the $(M_{\rm bc}, \Delta E, \mathcal{R})$ signal region. The results are $\mathcal{A} = 0.16 \pm 0.21$ and $\mathcal{S} = 0.19 \pm 0.30$, where the errors are statistical. The correlation coefficient is -0.10. These values are consistent with no *CP* violation ($\mathcal{A} = \mathcal{S} = 0$); the errors are consistent with MC expectations. Figure 3 shows the data and projections of the fit result.

The sources of systematic error are listed in Table I. The error for most sources is evaluated by varying the corresponding parameters by ± 1 standard deviation (σ). We vary the wrong tag fractions and the difference in these fractions between B^0 and $\bar{B}^0$ decays independently in each tag quality bin ℓ. The effect of a possible asymmetry in $b \to c$ and $q\bar{q}$ is evaluated by adding such an asymmetry to the $b \to c$ and $q\bar{q}$ Δt distributions. The uncertainty due to a possible asymmetry in $\rho\pi\pi$ nonresonant decays is esti-

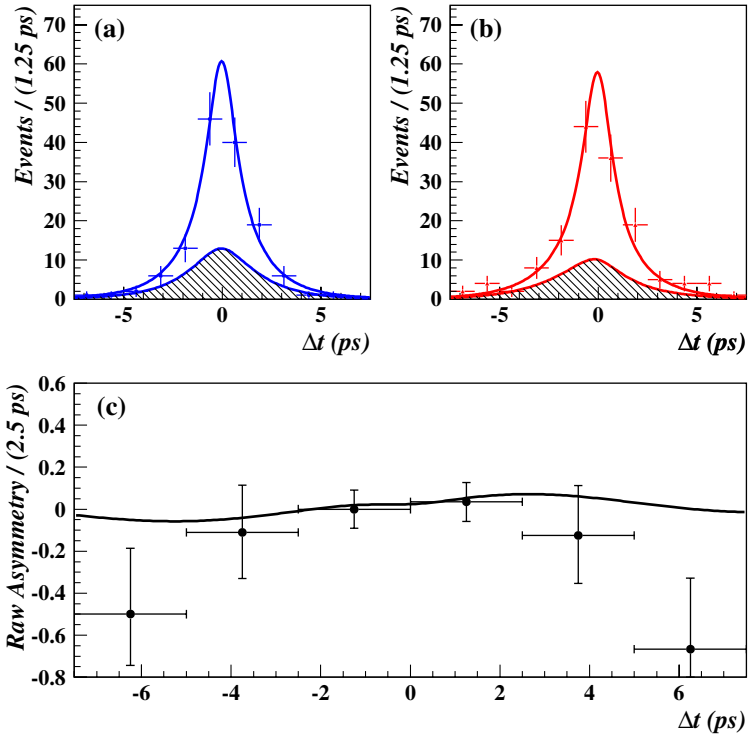

FIG. 3 (color online). The Δt distribution and projections of the fit for events satisfying $0.5 < r < 1.0$: (a) $Q = +1$ tags, (b) $Q = -1$ tags. The hatched region shows signal events. The raw *CP* asymmetry is shown in (c). For these plots the $\mathcal{R}$ requirement has been tightened to increase the ratio of signal to background.

TABLE I. Systematic errors for CP coefficients $\mathcal{A}$ and $\mathcal{S}$.

Type	$\Delta\mathcal{A}(\times 10^{-2})$ $+\sigma$	$-\sigma$	$\Delta\mathcal{S}(\times 10^{-2})$ $+\sigma$	$-\sigma$
Wrong tag fractions	0.5	0.5	0.8	0.8
Parameters Δm, τ_{B^0}	0.2	0.3	0.6	0.7
Resolution function	1.4	1.5	1.0	1.7
Background Δt distributions	0.5	0.5	1.0	1.1
Component fractions	1.5	1.9	3.9	3.7
$\rho\pi\pi$ nonresonant fractions	1.2	1.0	1.5	1.2
SCF fraction, Δt PDF	0.2	0.2	0.1	0.1
Shape of $\mathcal{R}$ PDF	0.8	0.7	1.2	1.3
Vertexing	2.1	2.1	1.0	1.3
Possible fitting bias	0.3	0.0	0.3	0.0
Background asymmetry	1.1	0.0	0.0	0.4
$b \to u$ asymmetry	2.4	2.9	2.4	3.2
$\rho\pi\pi$ asymmetry	4.6	4.6	4.6	4.6
Transverse polarization	3.8	2.8	4.6	2.7
Tag-side interference [16]	3.7	3.7	0.1	0.1
Total	8.3	8.0	8.4	7.9

mated by varying $\mathcal{A}_{\rho\pi\pi}$ and $\mathcal{S}_{\rho\pi\pi}$ by 0.68, corresponding to a 68% confidence interval of a free distribution. We vary the branching fractions for $a_1\rho$ and $a_1\pi$ decays and also allow for a CP asymmetry of up to 100% in these modes. The error due to transverse polarization is obtained by first setting f_L equal to its central value [6] and varying $\mathcal{A}_T, \mathcal{S}_T$ from -1 to $+1$; then, conservatively assuming that the transversely polarized component (with fraction $f_T = 1 - f_L$) is pure CP-odd for which $\mathcal{A}_T = \mathcal{A}_L, \mathcal{S}_T = -\mathcal{S}_L$, and varying f_L by its error. Summing up in quadrature all systematic uncertainties, we obtain overall systematic errors of ± 0.08 for both $\mathcal{A}$ and $\mathcal{S}$. Thus,

$$\mathcal{A} = 0.16 \pm 0.21(\text{stat}) \pm 0.08(\text{syst}) \tag{4}$$

$$\mathcal{S} = 0.19 \pm 0.30(\text{stat}) \pm 0.08(\text{syst}). \tag{5}$$

These values are consistent with, and supersede, our previous measurement [4]. They are also consistent with results obtained by *BABAR* [5].

We constrain ϕ_2 using an isospin analysis [17], which allows one to relate six observables to six underlying parameters: five decay amplitudes for $B \to \rho\rho$ and the angle ϕ_2. The observables are the branching fractions for $B \to \rho^+\rho^-$, $\rho^+\rho^0$ [6], and $\rho^0\rho^0$ [3]; the CP parameters $\mathcal{A}$ and $\mathcal{S}$ (our results); and the parameter $\mathcal{A}_{\rho^0\rho^0}$ for $B \to \rho^0\rho^0$ decays. The last parameter is not yet measured, but nevertheless one can constrain ϕ_2. The branching fractions must be multiplied by the corresponding longitudinal polarization fractions [6]. We neglect possible contributions from electroweak penguins and $I = 1$ amplitudes [18] and possible interference between signal and nonresonant components. We follow the statistical method of Ref. [19] and construct a $\chi^2(\phi_2)$ using the measured values and obtain a minimum χ^2 (denoted χ^2_{min}); we then scan ϕ_2 from 0° to 180°, calculating the difference $\Delta\chi^2 \equiv \chi^2(\phi_2) - \chi^2_{\text{min}}$. We insert $\Delta\chi^2$ into the cumulative distribution function for the χ^2 distribution for 1 degree of freedom to obtain a confidence level (C.L.) for each ϕ_2 value. The resulting function $1 - \text{C.L.}$ (Fig. 4) has more than one peak due to ambiguities that arise when solving for ϕ_2. The "flattop" regions in Fig. 4 arise because $\mathcal{A}_{\rho^0\rho^0}$ is not measured. The solution consistent with the standard model is $62° < \phi_2 < 106°$ at 68% C.L. or $54° < \phi_2 < 113°$ at 90% C.L. Recently, an alternative model-dependent approach to extract ϕ_2 using flavor $SU(3)$ symmetry has been proposed [20]. This method could potentially give more stringent constraints on ϕ_2.

In summary, we present an improved measurement of the CP-violating coefficients $\mathcal{A}$ and $\mathcal{S}$ in $B^0 \to \rho^+\rho^-$ decays using 492 fb^{-1} of data, which corresponds to 535×10^6 $B\bar{B}$ pairs. These measurements are used to constrain the angle ϕ_2.

We thank the KEKB group for the excellent operation of the accelerator, the KEK cryogenics group for the efficient operation of the solenoid, and the KEK computer group and the National Institute of Informatics for valuable computing and Super-SINET network support. We acknowledge support from the Ministry of Education, Culture, Sports, Science, and Technology of Japan and the Japan Society for the Promotion of Science; the Australian Research Council and the Australian Department of Education, Science and Training; the National Science Foundation of China and the Knowledge Innovation Program of the Chinese Academy of Sciences under Contracts No. 10575109 and IHEP-U-503; the Department of Science and Technology of India; the BK21 program of the Ministry of Education of Korea, the CHEP SRC program and Basic Research program (Grant No. R01-2005-000-10089-0) of the Korea Science and Engineering Foundation, and the Pure Basic Research

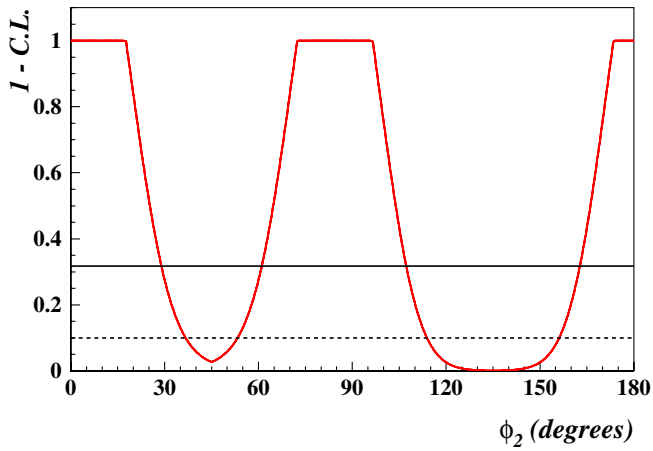

FIG. 4 (color online). $1 - \text{C.L.}$ vs ϕ_2. The horizontal lines denote C.L. = 68.3% (solid) and C.L. = 90% (dashed).

Group program of the Korea Research Foundation; the Polish State Committee for Scientific Research; the Ministry of Education and Science of the Russian Federation and the Russian Federal Agency for Atomic Energy; the Slovenian Research Agency; the Swiss National Science Foundation; the National Science Council and the Ministry of Education of Taiwan; and the U.S. Department of Energy.

[1] M. Kobayashi and T. Maskawa, Prog. Theor. Phys. **49**, 652 (1973); N. Cabibbo, Phys. Rev. Lett. **10**, 531 (1963).
[2] Charge-conjugate modes are included throughout this paper unless noted otherwise.
[3] B. Aubert *et al.* (*BABAR* Collaboration), Phys. Rev. Lett. **98**, 111801 (2007).
[4] A. Somov *et al.* (Belle Collaboration), Phys. Rev. Lett. **96**, 171801 (2006).
[5] B. Aubert *et al.* (*BABAR* Collaboration), Phys. Rev. Lett. **95**, 041805 (2005); Phys. Rev. Lett. **93**, 231801 (2004); arXiv:hep-ex/0607098.
[6] Heavy Flavor Averaging Group, August 2006, http://www.slac.stanford.edu/xorg/hfag/.
[7] A. Abashian *et al.* (Belle Collaboration), Nucl. Instrum. Methods Phys. Res., Sect. A **479**, 117 (2002).
[8] S. Kurokawa and E. Kikutani, Nucl. Instrum. Methods Phys. Res., Sect. A **499**, 1 (2003), and other papers in this volume.
[9] H. Kakuno *et al.*, Nucl. Instrum. Methods Phys. Res., Sect. A **533**, 516 (2004).
[10] G. C. Fox and S. Wolfram, Phys. Rev. Lett. **41**, 1581 (1978).
[11] S. H. Lee *et al.*, Phys. Rev. Lett. **91**, 261801 (2003).
[12] K.-F. Chen *et al.* (Belle Collaboration), Phys. Rev. D **72**, 012004 (2005); H. Tajima *et al.*, Nucl. Instrum. Methods Phys. Res., Sect. A **533**, 370 (2004).
[13] H. Albrecht *et al.* (Argus Collaboration), Phys. Lett. B **241**, 278 (1990).
[14] B. Aubert *et al.* (*BABAR* Collaboration), Phys. Rev. Lett. **97**, 051802 (2006); K. Abe *et al.* (Belle Collaboration), arXiv:hep-ex/0507096.
[15] B. Aubert *et al.* (*BABAR* Collaboration), Phys. Rev. D **74**, 031104 (2006).
[16] O. Long *et al.*, Phys. Rev. D **68**, 034010 (2003).
[17] M. Gronau and D. London, Phys. Rev. Lett. **65**, 3381 (1990).
[18] A. Falk *et al.*, Phys. Rev. D **69**, 011502(R) (2004).
[19] J. Charles *et al.* (CKMfitter Group), Eur. Phys. J. C **41**, 1 (2005).
[20] M. Beneke, M. Gronau, J. Rohrer, and M. Spranger, Phys. Lett. B **638**, 68 (2006).